Inorganic Chemistry

Article

pubs.acs.org/IC

Synthesis and Physical Properties of $K_4[Fe(C_5O_5)_2(H_2O)_2](HC_5O_5)_2{\cdot}4H_2O$ ($C_5O_5^{2-}$ = Croconate): A Rare Example of Ferromagnetic Coupling via H-bonds

Matteo Atzori,[†] Elisa Sessini,[†] Flavia Artizzu,[†] Luca Pilia,[†] Angela Serpe,[†] Carlos J. Gómez-García,[‡] Carlos Giménez-Saiz,[‡] Paola Deplano,[†] and Maria Laura Mercuri*[,†]

[†]Dipartimento di Scienze Chimiche e Geologiche, Università degli Studi di Cagliari, S.S. 554−Bivio per Sestu−I09042 Monserrato (Cagliari), Italy

[‡]Instituto de Ciencia Molecular (ICMol) Parque Científico, Universidad de Valencia, 46980 Paterna (Valencia), Spain

Supporting Information

ABSTRACT: The reaction of the croconate dianion $(C_5O_5)^{2-}$ with a Fe(III) salt has led, unexpectedly, to the formation of the first example of a discrete Fe(II)−croconate complex without additional coligands, $K_4[Fe(C_5O_5)_2(H_2O)_2](HC_5O_5)_2{\cdot}4H_2O$ (**1**). **1** crystallizes in the monoclinic $P2_1/c$ space group and presents discrete octahedral Fe(II) complexes coordinated by two chelating $C_5O_5^{2-}$ anions in the equatorial plane and two trans axial water molecules. The structure can be viewed as formed by alternating layers of *trans*-diaquabis(croconato)ferrate(II) complexes and layers containing the monoprotonated croconate anions, $HC_5O_5^-$, and noncoordinated water molecules. Both kinds of layers are directly connected through a hydrogen bond between an oxygen atom of the coordinated dianion and the protonated oxygen atom of the noncoordinated croconate monoanion. A H-bond network is also formed between the coordinated water molecule and one oxygen atom of the coordinated croconate. This H-bond can be classified as strong−moderate being the O···O bond distance (2.771(2) Å) typical of moderate H-bonds and the O−H···O bond angle (174(3)°) typical of strong ones. This H-bond interaction leads to a quadratic regular layer where each $[Fe(C_5O_5)_2(H_2O)_2]^{2-}$ anion is connected to its four neighbors in the plane through four equivalent H-bonds. From the magnetic point of view, these connections lead to an $S = 2$ quadratic layer. The magnetic properties of **1** have been reproduced with a 2D square lattice model for $S = 2$ ions with $g = 2.027(2)$ and $J = 4.59(3)$ cm^{-1}. This model reproduces quite satisfactorily its magnetic properties but only above the maximum. A better fit is obtained by considering an additional antiferromagnetic weak interlayer coupling constant (j) through a molecular field approximation with $g = 2.071(7)$, $J = 2.94(7)$ cm^{-1}, and $j = -0.045(2)$ cm^{-1} (the Hamiltonian is written as $H = -JS_iS_j$). Although this second model might still be improved since there is also an extra contribution due to the presence of ZFS in the Fe(II) ions, it confirms the presence of weak ferromagnetic Fe−Fe interactions through H-bonds in compound **1** which represents one of the rare examples of ferromagnetic coupling via H-bonds.

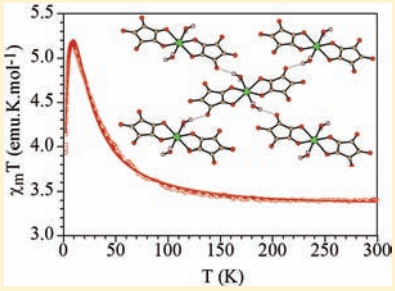

INTRODUCTION

The croconato ligand ($C_5O_5^{2-}$ = dianion of croconic acid = 4,5-dihydroxycyclopent-4-ene-1,2,3-trione) is the $n = 5$ member of the cyclic oxocarbons of formula $C_nO_n^{2-}$ ($n = 3-6$ for deltate, squarate, croconate, and rhodizonate anions, respectively), the aromatic series which is stabilized by electron-delocalization of π-electrons over the ring. The croconato ligand, due to its potential coordination modes toward a wide variety of transition metal ions, through the five oxygen donor atoms, can be used to obtain complexes with different molecular structures showing nD supramolecular architectures ($n = 1-3$), where H-bonding may play a role in determining their 2D or 3D dimensionality. Moreover, the croconato ligand may act either as bridging ligand, opening new perspectives into the design and synthesis of new heterometallic assemblies with interesting magnetic and optical properties or as building block for the synthesis of multifunctional molecular materials.[1−3] The properties of this very versatile ligand, its ability to mediate magnetic interactions (similarly to the oxalato ligand),[1−3] and its coordination modes toward first row transition divalent metals have been widely described by Julve et al.[4] Its coordinating behavior has been subject of thorough research efforts which have led to the identification of a wide variety of bonding modes in metal complexes (see Scheme 1): terminal bidentate (I),[5,6] bridging bis-bidentate (II and III),[4b,5b,7,8] bridging bis-bidentate/monodentate (IV and V),[9] bis-bidentate/monodentate through the five (VI)[10] ligand oxygen donor atoms, bis-bidentate/monodentate (IX)[11a] or bis-bidentate/bis-monodentate with either cis (VIII)[11b] or trans (IX)[11a] arrangements through four oxygen atoms, bidentate/bis-monodentate (X and XI)[11b,12] through three adjacent croconate-oxygen atoms, and tris-bidentate (XII).[7d,8b] Recently, the unprecedented μ-1,2-bis(monodentate) coordination mode

Received: February 14, 2012
Published: April 24, 2012

   dx.doi.org/10.1021/ic300331e | *Inorg. Chem.* 2012, 51, 5360−5367

Scheme 1. Coordination Modes of the Croconato Ligand in Metal Complexes

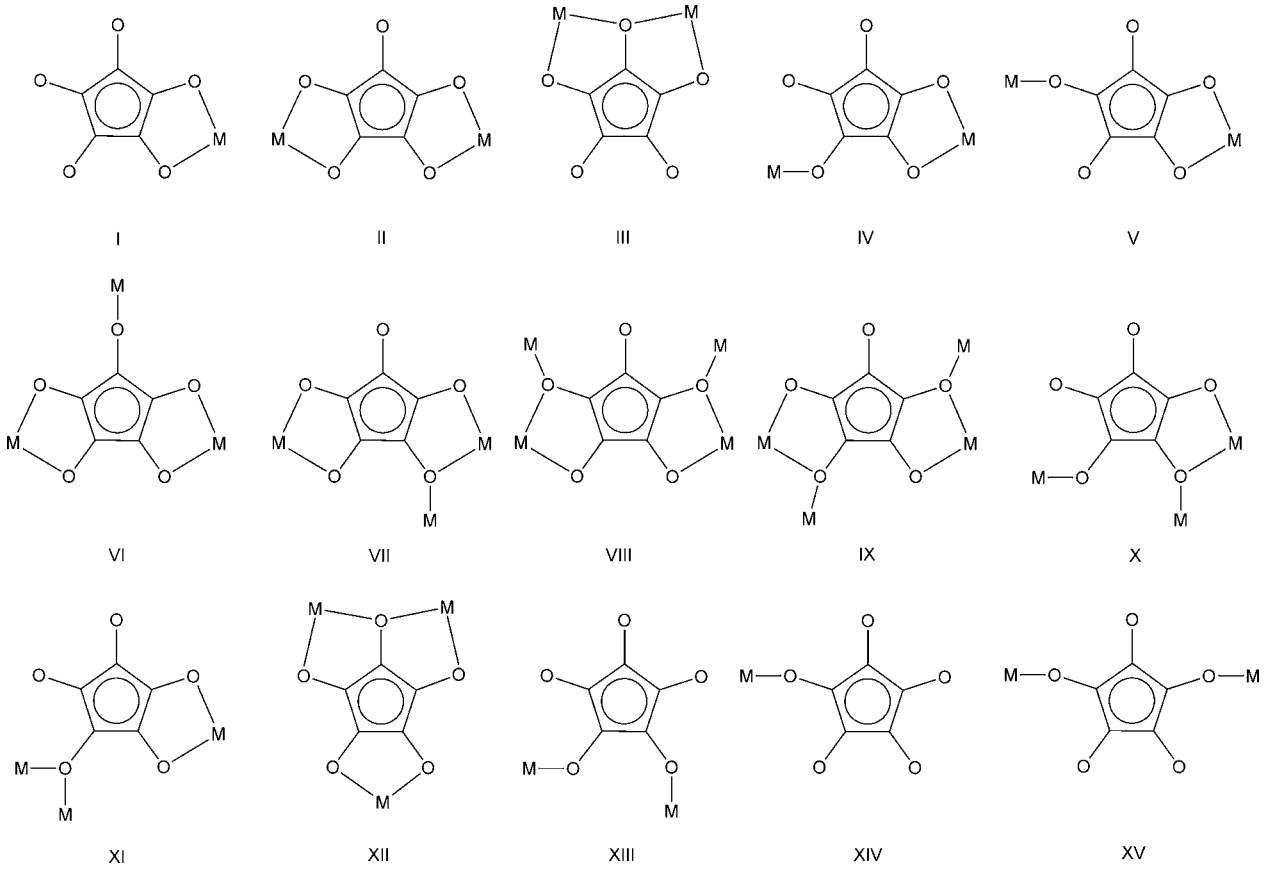

of the croconato dianion toward Mn(II) and Cu(II) has been reported (structure XIII in Scheme 1).[13] In the case of lanthanide metal ions, a variety of molecular arrangements have been observed, where the ligand coordination modes ranges from chelating or bis-chelating for Ce(III)−Gd(III) metal ions (structures I and II in Scheme 1) to monodentate or bis-monodentate (XIV, XV) in the case of trivalent ions belonging to the second half of the lanthanide series (Tb, Dy, Ho, Er, Yb).[14]

We have recently obtained and fully characterized the $[A]_3[M(C_5O_5)_3]$ (A = *n*-Bu_4N^+, Ph_4P^+; M = Fe(III), Ga(III)) salts, the first examples of tris-chelated metal(III) complexes containing the novel mononuclear tris(croconato)metalate(III) chiral anions[15] and two new molecular paramagnetic conductors with the tris(croconato)ferrate(III) anion and the BEDT-TTF as organic donor: α-$(BEDT\text{-}TTF)_5[Fe(C_5O_5)_3]\cdot 5H_2O$, which is probably the first paramagnetic semiconductor with a chirality-induced α-phase and ß-$(BEDT\text{-}TTF)_5[Fe(C_5O_5)_3]\cdot C_6H_5CN$, one of the rare examples of paramagnetic molecular metals.[6]

With the aim of preparing new croconato-based complexes to be used as magnetic building blocks for the synthesis of novel multifunctional molecular materials, we report herein the synthesis and physical characterization of $K_4[Fe(C_5O_5)_2(H_2O)_2](HC_5O_5)_2\cdot 4H_2O$ (**1**), the first discrete Fe(II)-croconate complex without additional coligands[9a,16] showing a peculiar magnetic exchange pathway through H-bonds.[16b]

EXPERIMENTAL SECTION

General Remarks. $K_2C_5O_5$ was been synthetized according to literature method.[17] $FeCl_3$ was used as received from Aldrich. FT-IR spectrum was performed on KBr pellets and collected with a Bruker Equinox 55 spectrophotometer. The magnetic susceptibility measurements were carried out in the temperature range 2−300 K with an applied magnetic field of 0.1 T on a polycrystalline sample of compound **1** (59.45 mg) with a Quantum Design MPMS-XL-5 SQUID susceptometer. The isothermal magnetization was performed on the same sample at 2 K with magnetic fields up to 8 T with a Quantum Design PPMS-9 equipment. The susceptibility data were corrected for the sample holder previously measured using the same conditions and for the diamagnetic contributions of the salt as deduced by using Pascal's constant tables ($\chi_{dia} = -378.8 \times 10^{-6}$ emu mol^{-1}).[18] C, H, and N analyses were performed with a Carlo Erba mod. EA1108 CHNS analyzer.

Synthesis of $K_4[Fe(C_5O_5)_2(H_2O)_2](HC_5O_5)_2\cdot 4H_2O$ (1). An aqueous solution of 0.063 g (0.385 mmol) of $FeCl_3$ was added dropwise to a hot aqueous solution of 0.252 g (1.15 mmol) of $K_2C_5O_5$. The resulting solution was left stirring at ca. 60 °C. After 30 min, the dark solution was allowed to cool down slowly and a brown-violet solid precipitates. It was filtrated and washed with cold distilled water, a mixture of H_2O/EtOH, EtOH, and finally Et_2O. Dark-violet shiny crystals suitable for X-ray analysis were collected after slow evaporation of the mother liquor for several days (54% yield); Elemental anal. calc. for $C_{20}H_{14}FeK_4O_{26}$: C, 27.38%; H, 1.55%. Found: C, 27.22%; H, 1.60%. FT-IR (ν_{max}/cm^{-1}, KBr pellet): 3516 m, 3461 w, 3360 m, 3217 m, 1873 w, 1750 w, 1722 m, 1683 vw, 1648 m, 1629 m, 1513 vs-br, 1356 s, 1282 m, 1243 w, 1222 w, 1191 w, 1112 w, 1093 w, 995 m, 844 m, 638 m, 592 m, 560 m, 544 vw, 528 w, 502 vw, 425 s.

Data Collection and Structure Determination. X-ray diffraction data of compound **1** were collected at 180(2) K with a Nonius Kappa CCD diffractometer using a graphite monochromated Mo$K\alpha$ radiation source (α = 0.71073 Å). Denzo and Scalepack[19] programs

dx.doi.org/10.1021/ic300331e | *Inorg. Chem.* 2012, 51, 5360−5367

were used for cell refinements and data reduction. The structure was solved by direct methods using the SIR97[20] program with the WinGX[21] graphical user interface. The structure refinement was carried out with SHELX-97.[22] A multiscan absorption correction, based on equivalent reflections was applied to the data using the program SORTAV.[23] Water H atoms and the H atom of the monoprotonated croconate anion were found in difference maps and refined positionally without the use of any geometrical restraints. All non-hydrogen atoms were refined anisotropically. Crystallographic data are summarized in Table 1. The powder X-ray pattern of the same sample that was measured in the SQUID has been checked, and it corresponds with the simulated X-ray spectrum from the single crystal X-ray structure. Both spectra are reported in Figure S2 in the Supporting Information.

Table 1. Summary of X-ray Crystallographic Data for 1

compound	1
empirical formula	$C_{20}H_{14}FeK_4O_{26}$
formula weight	882.56
crystal size, mm	0.4 × 0.3 × 0.3
crystal system	monoclinic
space group	$P2_1/c$
a, Å	10.07260(15)
b, Å	14.8747(2)
c, Å	10.1921(2)
α, deg	90
β, deg	107.6734(6)
γ, deg	90
V, Å^3	1454.98(4)
Z	2
T, K	180(2)
ρ(calc), Mg m^{-3}	2.015
μ, mm^{-1}	1.206
θ range, deg	2.12−31.04
GooF	1.017
$R1$ [$I > 2\sigma(I)$]	0.0426
$wR2$ [$I > 2\sigma(I)$]	0.0907

RESULTS AND DISCUSSION

Synthesis of $K_4[Fe(C_5O_5)_2(H_2O)_2](HC_5O_5)_2{\cdot}4H_2O$ (1). The synthesis of compound $K_4[Fe(C_5O_5)_2(H_2O)_2](HC_5O_5)_2{\cdot}4H_2O$ (**1**) has been carried out, as described in detail in the Experimental Section, according to the following reaction scheme (Scheme 2).

Interestingly, although we started from a Fe(III) salt, Fe(II) is found in compound **1**, as shown by the Fe−O bond lengths (see below). Since there is no other reducing agent in the reaction medium, the only possibility is that a fraction of the croconate anions acts as a reducing agent. It has been shown since 1982 by Fatiadi and Doane,[24] and more recently by Fabre et al.,[25] that the croconate anion and its derivatives croconate violet and croconate blue, called pseudo-oxocarbons, show two reversible oxidation steps at relatively low potential values, confirming their reducing character. In particular, for the croconate anion the oxidation potentials measured versus SCE in DMF[26] associated to the following redox reactions are

$$C_5O_5^{2-} \rightleftharpoons C_5O_5^{\bullet -} + e^- \qquad E^1_{1/2} = 0.11\ V$$

$$C_5O_5^{\bullet -} \rightleftharpoons C_5O_5 + e^- \qquad E^2_{1/2} = 0.45\ V$$

This means that the croconate dianion can be easily oxidized to the radical anion $[C_5O_5]^{\bullet -}$ with a standard potential of 0.381 V versus SHE in DMF, below the Fe(III)/Fe(II) standard potential (0.771 V versus SHE). Thus, it is not surprising that the Fe(III) ions might be reduced to Fe(II) while the croconate dianion $[C_5O_5]^{2-}$ is oxidized to the radical anion $[C_5O_5]^{\bullet -}$, as already observed with croconate violet and Fe(III) by Fabre et al.[27]

It is noteworthy that in the synthesis of the $[A]_3[Fe(C_5O_5)_3]$ (A = n-Bu_4N^+, Ph_4P^+) salts,[15a] a Fe(III)/Fe(II) reduction was not observed and this could be related to the different synthetic procedure. In that case, the products were obtained immediately as brown solids partially soluble in water, then recrystallized from a mixture of organic solvents. In the present case, instead, we have obtained compound **1** directly from the mother liquor only after a slow evaporation of the solvent.

Crystal Structure of $K_4[Fe(C_5O_5)_2(H_2O)_2](HC_5O_5)_2{\cdot}4H_2O$ (1). **1** crystallizes in the monoclinic space group $P2_1/c$ (Table 1). The asymmetric unit of **1** comprises half *trans*-diaquabis(croconato)ferrate(II) dianion, one monoprotonated croconate monoanion, two potassium cations, and two water molecules of crystallization (Figure 1). The iron atom is located on a

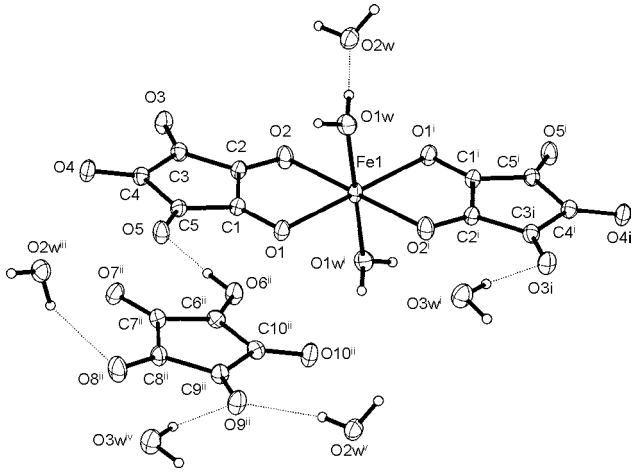

Figure 1. ORTEP view showing the molecules present in the crystal structure of **1** and some of the hydrogen bonds (dotted lines). Thermal ellipsoids are drawn at the 50% probability level. Symmetry codes: (i) $-x + 1, -y, -z + 1$; (ii) $x, -y + 1/2, z - 1/2$; (iii) $-x + 1, y + 1/2, -z + 1/2$; (iv) $x - 1, -y + 1/2, z - 3/2$; (v) $x - 1, y, z - 1$.

Scheme 2. Synthesis of 1

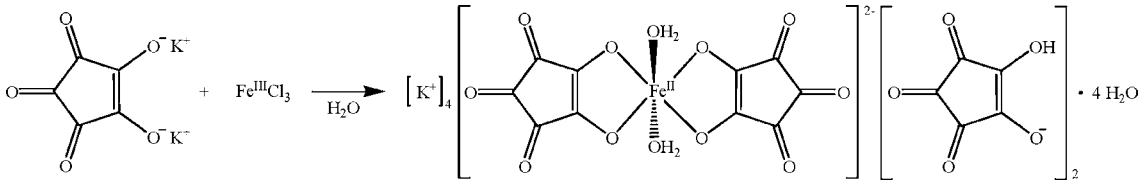

dx.doi.org/10.1021/ic300331e | Inorg. Chem. 2012, 51, 5360−5367

crystallographic inversion center and is six-coordinated with four coplanar oxygen atoms from two croconato ligands in the equatorial plane (with Fe−O_{croc} bond distances of 2.1383(14) and 2.2225(15) Å), whereas the axial positions are occupied by two water molecules (with a Fe−O1W bond distance of 2.0787(16) Å). The croconate anion acts as a bidentate ligand toward the Fe(II) ion with a bite O1−Fe−O2 angle of 80.71(6)°. These equatorial Fe−O bond distances and the bite O−Fe−O angle are similar to those observed in the other three known Fe(II)-croconate complexes (2.156−2.215 Å and 80.35° in GOFZEG,[16a] 2.155−2.274 Å and 77.38−79.13° in ISIKOK,[16b] and 2.134−2.202 Å and 79.17° in YAYVEZ) (Table 2).[9a,16c]

Table 2. Fe−O Bond Distances (Å) and O−Fe−O Bite Angles (deg) in the Reported Croconate Compounds with Fe(II) and Fe(III)

compound	oxidation state	Fe−O	O−Fe−O	ref
1	Fe(II)	2.1833−2.2225	80.71	this work
GOFZEG	Fe(II)	2.156−2.215	80.35	16a
ISIKOK	Fe(II)	2.155−2.274	77.38−79.13	16b
YAYVEZ	Fe(II)	2.134−2.202	79.17	9a, 16c
CETNAR	Fe(III)	2.001−2.057	82.16−83.14	6
CETNEV	Fe(III)	2.038−2.046	82.17−82.22	6
KEFLOX	Fe(III)	2.009−2.044	80.88−82.45	15
KEFLUD	Fe(III)	2.008−2.062	81.98−82.37	15

Note also that these Fe−O_{croc} bond distances are significantly longer than those found in the four known $[Fe(C_5O_5)_3]^{3-}$ compounds, where the Fe−O bond distances are in the range 2.001−2.057 Å in CETNAR,[6] 2.038−2.046 Å in CETNEV,[6] 2.009−2.044 Å in KEFLOX,[15] and 2.008−2.062 in KEFLUD.[15] (Table 2). As expected, the shorter Fe−O_{croc} bond distances in the $[Fe(C_5O_5)_3]^{3-}$ compounds give rise to larger bite angles: 82.16−83.14° in CETNAR,[6] 82.17−82.22° in CETNEV,[6] 80.88−82.45° in KEFLOX,[15] and 81.98−82.37° in KEFLUD[15] (Table 2). All these data confirm the +2 oxidation state for the Fe atom in complex **1**.

The C−C and C−O bond distances for the croconate anions are listed in Table 3. As expected, the longer C−O distances in the croconate dianion, $C_5O_5^{2-}$ are associated to the oxygen atoms that are coordinated to the metal (O1 and O2) and the shortest C−C bond corresponds to the expected position of the double bond in the ring, i.e. C1−C2 (see Scheme 3a), suggesting a greater negative charge concentration on the

Table 3. C−C and C−O Distances for the Croconato Anions in Compound 1 (Å)

$(C_5O_5)^{2-}$		$(HC_5O_5)^{-}$	
C1−O1	1.258(2)	C6−O6	1.313(3)
C2−O2	1.254(3)	C7−O7	1.231(3)
C3−O3	1.237(2)	C8−O8	1.231(3)
C4−O4	1.236(2)	C9−O9	1.231(3)
C5−O5	1.255(3)	C10−O10	1.243(3)
C1−C2	1.448(3)	C6−C7	1.432(3)
C2−C3	1.468(3)	C7−C8	1.488(3)
C3−C4	1.490(3)	C8−C9	1.484(3)
C4−C5	1.475(3)	C9−C10	1.491(3)
C5−C1	1.447(3)	C10−C6	1.432(3)

Scheme 3. Negative Charge Localization in (a) Croconate Dianion and (b and c) Monoprotonated Croconic Acid

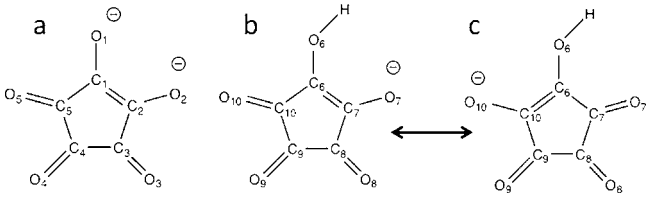

oxygen atoms linked to the metal. This is confirmed by the different C−C bond lengths in each ligand ring; in fact, the ones closer to the metal are shorter than the remaining ones suggesting that the croconate ring maintains an idealized local C_{2v} symmetry, as found in the croconic acid (Scheme 3a, Table 3).[15b] On the other hand, in the monoprotonated croconate anion, $HC_5O_5^-$, the longest C−O distance clearly corresponds to the oxygen bearing the H atom (O6), while all the other four C−O bonds have similar distances, indicating that the negative charge is shared between them (O7, O8, O9, and O10) (see Scheme 3b and 3c). This is confirmed by the similar C−C bond distances of C6−C7 and C6−C10 (indicating that the double bond is delocalized between these two positions) which in turn are shorter than the other three C−C distances in the ring.

The structure can be viewed as formed by alternating layers of *trans*-diaquabis(croconato)ferrate(II) complexes and layers containing the monoprotonated croconate anions and non-coordinated water molecules, labeled as O2W (Figure 2). Both

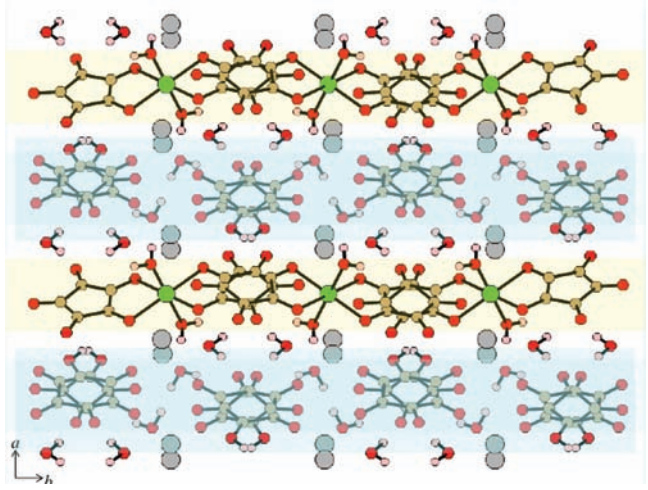

Figure 2. Perspective view of the structure of **1** in the *ab* plane. The yellow band indicates the layers containing the iron complexes: (color code) C = brown, H = pink, K = gray, and O = red.

kinds of layers are directly connected through a hydrogen bond formed between an oxygen atom of the coordinated anion (O5) and the protonated oxygen atom (O6) of the noncoordinated croconate anion (Figure 1). There is also an interlayer indirect connection through one water molecule that forms hydrogen bonds with both layers (O3W−H3A···O3 and O3W−H3B···O9) (see Table 4 for hydrogen bond distances and angles). Potassium cations also connect both types of layers as they are coordinated by oxygen atoms belonging to both layers and some water molecules. K1 and K2 are coordinated by eight oxygen atoms at distances lower than 3.1 Å.

dx.doi.org/10.1021/ic300331e | *Inorg. Chem.* 2012, 51, 5360−5367

Table 4. Hydrogen Bonds for 1 (Å and deg)

D−H···A	*d*(D−H)	*d*(H···A)	d(D···A)	<(DHA)
O6−H6···O5[a]	0.89(4)	1.67(4)	2.558(2)	176(3)
O1W−H1A···O3[b]	0.80(3)	1.97(3)	2.771(2)	174(3)
O1W−H1B...O2W	0.82(3)	1.76(3)	2.575(2)	171(3)
O2W−H2A···O9[c]	0.79(3)	2.00(3)	2.767(2)	167(3)
O2W−H2B···O8[d]	0.88(4)	2.13(4)	2.866(3)	140(3)
O2W−H2B···O7[e]	0.88(4)	2.42(4)	2.947(2)	118(3)
O3W−H3A···O3	0.88(4)	2.09(4)	2.966(2)	174(3)
O3W−H3B···O9[f]	0.89(4)	2.13(4)	3.017(2)	170(3)

[a]Symmetry codes: *x*, −*y* + 1/2, *z* + 1/2. [b]*x*, −*y* + 1/2, *z* − 1/2. [c]*x* + 1, −*y* + 1/2, *z* + 1/2. [d]−*x* + 1, −*y*, −*z* + 1. [e]*x* + 1, *y*, *z*. [f]*x* + 1, *y*, *z* + 1.

Figure 3 shows a fragment of the layer containing the iron complexes. Within this layer, each complex is linked to other

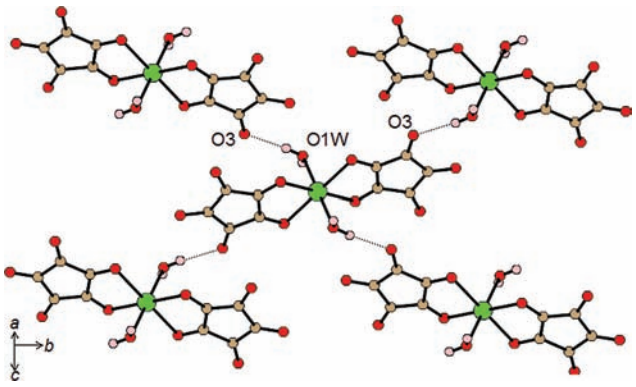

Figure 3. Perspective view of the $[Fe(C_5O_5)_2(H_2O)_2]^{2-}$ complexes in **1** and their intralayer H-bonds (dotted lines): (color code) C = brown, H = pink, and O = red.

four complexes through hydrogen bonds formed between the coordinated water molecules and one oxygen atom of the croconate ligand (O1W−H1A···O3).

Figure 4 shows the layer containing the monoprotonated croconate anions. Within this layer, one of the water molecules forms hydrogen bonds to oxygen atoms belonging to different monoprotonated croconate anions: one of them is O2W−H2A···O9 and the other is a bifurcated hydrogen bond from the donor group O2W−H2B to oxygen atoms O7 and O8 (see Figure 4 and Table 4). Finally, the O2W water molecule also

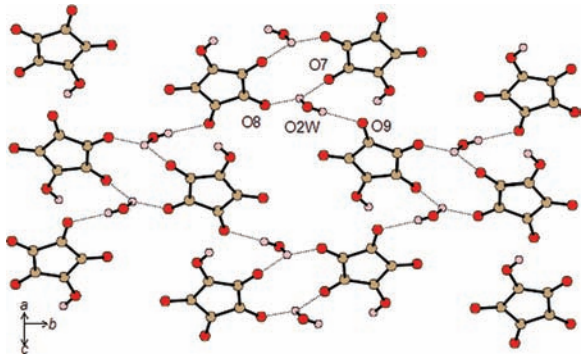

Figure 4. Perspective view of the layer containing the monoprotonated croconate anions and the noncoordinated water molecules. Hydrogen bonds are shown as dotted lines: (color code) C = brown, H = pink, and O = red.

acts as a hydrogen bond acceptor with the coordinating water molecule (O1W) of a neighboring layer (O1W−H1B···O2W).[28]

Recently Horiuchi et al. have discovered strong ferroelectric behavior above room temperature in a crystal of croconic acid,[29] which in its crystalline form consists of polar stacks of sheets of hydrogen-bonded molecules. The layers of monoprotonated croconic acid, which are present in the structure, suggest that compound **1** might show ferroelectricity with proton transfer to a hydrogen-bonded neighbor by application of an electric field.

Spectroscopic Characterization. *Vibrational Spectroscopy.* The infrared spectrum of **1** (reported in Figure S1 in the Supporting Information) exhibits characteristic bands of the croconato moiety. According to West et al.[30] the bands found at 1750, 1722, and 1683 cm^{-1} in the FT-IR spectrum can be assigned to the stretching vibrations of uncoordinated carbonyl groups which exhibit a double bond character, in agreement with structural findings. The IR band centered at 1638 cm^{-1} can be assigned, instead, to the stretching vibrations of coordinated carbonyls. The observed split at 1624−1589 cm^{-1} for this band may be attributed to the coordination of these groups to Fe(II) and K^+. The strong and broad band centered at 1513 cm^{-1} is assigned to the combination band of the stretching vibrations C−O and C−C typically observed for $C_nO_n^{2-}$ dianions salts or complexes. In the FT-IR spectrum of **1** there are also four bands in the 3600−3000 cm^{-1} region that can be assigned to the stretching vibrations of the different O−H bonds present in the structure: O−H bonds of coordination and crystallization water molecules and O−H bonds of monoprotonated croconic acids.

Magnetic Properties. The thermal variation of the molar magnetic susceptibility per Fe(II) ion times the temperature ($\chi_m T$) for compound **1** shows at room temperature a value of ca. 3.4 emu K mol^{-1}, which is the expected one for an isolated high spin Fe(II) ion (S = 2) with a g value of ca. 2.13 (Figure 5). When cooling down the sample, the $\chi_m T$ product remains

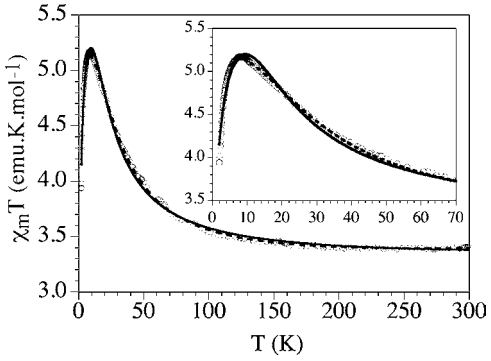

Figure 5. Thermal variation of the $\chi_m T$ product per Fe(II) ion for compound **1**. Solid and dashed lines show the best fit to the models (see text).

constant down to ca. 100 K, and below this temperature, it shows a progressive increase to reach a maximum of ca. 5.2 emu K mol^{-1} at ca. 9 K (Figure 5). Below 9 K, the $\chi_m T$ product shows a sharp decrease to reach a value of ca. 3.9 emu K mol^{-1} at 2 K. This behavior suggests that compound **1** presents a predominant weak ferromagnetic coupling, responsible of the increase below ca. 100 K. The decrease at low temperatures

dx.doi.org/10.1021/ic300331e | *Inorg. Chem.* 2012, 51, 5360−5367

may be indicative of a weak antiferromagnetic coupling and/or of the presence of a zero field splitting on the Fe(II) ions.

Although the structure of this compound presents layers of $[Fe(C_5O_5)_2(H_2O)_2]^{2-}$ anions where the Fe(II) ions are quite well isolated, a close look at the H bonds in this layer (Figure 3) shows the presence of a H-bond network formed between the coordinated water molecule and one oxygen atom of the coordinated croconate unit: (O1W−H1A···O3, Table 3). This H-bond can be classified as strong−moderate after the definition of Steiner[31] since although the O···O bond distance (2.771(2) Å) is typical of moderate H-bonds, the O−H···O bond angle (174(3)°) is typical of strong ones. This H-bond interaction leads to a quadratic regular layer where each $[Fe(C_5O_5)_2(H_2O)_2]^{2-}$ anion is connected to its four neighbors in the plane through four equivalent O1W−H1A···O3 bonds. From the magnetic point of view these connections lead to an $S = 2$ quadratic layer. Given the size of the local interacting spins ($S = 2$), we can consider them as classical spins and, therefore, we can use the classical spin quadratic layer developed by Curély for Heisenberg systems.[32] For compound **1**, we can consider a perfect quadratic layer with only one coupling constant, J, and only one g value. This simplification leads to the following equation for the Curély model:

$$\chi_{2D} = \frac{N\beta^2 g^2}{3kT} S(S+1) \frac{g^2 W_1 + g^2 W_2}{(1-u^2)^2} \quad (1)$$

being $W_1 = (1+u^2)^2 + 4u^2$, $W_2 = 2u(1+u^2) + 2u(1+u^2)$, and $u = \coth[JS(S+1)/kT] - (kT/JS(S+1))$.

This model reproduces quite satisfactorily the magnetic properties of compound **1** but only above the maximum with $g = 2.027(2)$ and $J = 4.59(3)$ cm^{-1} (dashed line in Figure 5; the Hamiltonian is written as $H = -J\sum(S_iS_j)$, being S_iS_j all the possible nearest neighbors spins couplings). In order to reproduce the decrease observed in $\chi_m T$ at low temperatures, we have to include either a zero-field splitting (ZFS) contribution or the presence of a weak antiferromagnetic coupling. The first of these contributions can be included by modifying the 2D susceptibility given by eq 1 with a perturbational approach.[33] Unfortunately, this approach does not give rise to realistic parameters nor reproduces satisfactorily the magnetic data. A possible reason to explain this failure may be the high correlation between the magnetic coupling and the zero-field splitting parameters which must be small and present similar contributions.

A second possibility to reproduce the decrease observed at low temperatures is the presence of an weak interplane antiferromagnetic interaction. This contribution can be included by using the mean field approximation:[34]

$$\chi = \frac{\chi_{2D}}{1 - (2zj/Ng^2\beta^2)\chi_{2D}} \quad (2)$$

where j is the interplane coupling constant with the z neighbors and χ_{2D} is the susceptibility of the quadratic layer given by eq 1. This model reproduces quite satisfactorily the magnetic properties of compound **1** in the whole temperature range (solid line in Figure 5) with $g = 2.071(7)$, $J = 2.94(7)$ cm^{-1}, and $zj = -0.09(1)$ cm^{-1}. Note that the parameters obtained with this approximation are more realistic and the model reproduces quite well the magnetic data at low temperatures, although the maximum in the $\chi_m T$ plot is not perfectly reproduced (inset in Figure 5). A possible reason to explain this difference may be the simultaneous presence of both, a ZFS in the Fe(II) ions together with a weak antiferromagnetic interplane coupling. Unfortunately, a model including all these contributions is not available and would include too many correlated parameters that would lead to a scantily reliable result.

Although weak, the main magnetic coupling is clearly ferromagnetic, as evidenced by the increase in the $\chi_m T$ product when cooling the sample and also in agreement with the J value found in both fits. This weak ferromagnetic coupling can only be attributed to the presence of moderate−strong H-bonds, as already mentioned. Although not very common, the existence of a ferromagnetic coupling through moderate-strong H-bonds has already been observed in two Mn(III) malonate complexes presenting very similar layered structures.[33] Furthermore, in a very interesting study, Ruiz et al. have clearly shown with theoretical density functional theory (DFT) calculations that H-bonds can promote weak ferromagnetic coupling.[35] In our case, the magnetic coupling, although weak, is higher that the one observed in the mentioned Mn(III) compounds, even if the H-bond parameters are very similar. A possible reason to explain our higher values may be the absence of any Jahn−Teller elongation in compound **1**, in contrast to the Mn(III) (d^4) complexes, where this elongation is clearly evidenced by the long axial Mn−O(w) bond distances (2.245(6) and 2.268(6) Å) which are much longer than the corresponding axial Fe−O(w) bond distances in compound **1** (2.0787(16) Å). This longer M−O(w) bond distance in the Mn(III) derivatives is expected to lead to much weaker overlaps of the magnetic orbitals and, consequently, to a much weaker magnetic coupling, as clearly described by Julve et al.[33]

A confirmation of the weak ferromagnetic coupling found in compound **1** and of the weak antiferromagnetic coupling (or ZFS) observed at lower temperatures is provided by the isothermal magnetization at 2 K that shows a behavior close to the expected one for an isolated high spin ($S = 2$) Fe(II) ion (Figure 6). However, the corresponding Brillouin function for

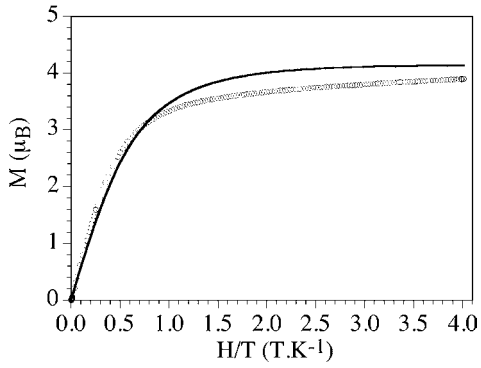

Figure 6. Isothermal magnetization at 2 K for compound **1**. The solid line represents the Brillouin function for an $S = 2$ ion with $g = 2.071$.

an $S = 2$ ion with $g = 2.071$ (solid line in Figure 6) is slightly below the experimental data at low fields, suggesting the presence of a weak ferromagnetic coupling. As a result of this ferromagnetic coupling, the experimental points reach saturation before (i. e., at lower fields) than the Brillouin function for a perfect paramagnet. Albeit, the presence of an additional antiferromagnetic coupling (and/or a ZFS in the Fe(II) ion) reduces the expected saturation value, and therefore, the experimental data saturate at a lower value than the calculated one (and, therefore, cross the calculated line; Figure 6).

dx.doi.org/10.1021/ic300331e | Inorg. Chem. 2012, 51, 5360−5367

CONCLUSIONS

$K_4[Fe(C_5O_5)_2(H_2O)_2][C_5O_5H]_2{\cdot}4H_2O$ (**1**) represents one of the very few examples of Fe(II)−croconate complexes and the first discrete one without additional ligands. Furthermore, **1** is the first reported Fe(II)−croconate complex prepared from Fe(III) and shows the ability of the croconate anion to act as a Fe(III)/Fe(II) reducing agent (at least in the synthetic conditions used in this work). Interestingly, **1** presents an extended network of moderate−strong H-bonds that leads to the formation of quadratic layers that represent one of the very few examples of ferromagnetic coupling mediated through H-bonds. Therefore its preparation opens the door to the synthesis of novel Fe(II) complexes as magnetic components of multifunctional molecular materials with peculiar magnetic properties: in fact, the removal of the axial water molecules and the use of an appropriate bridging ligand or complex may lead to regular or alternating magnetic chains.

ASSOCIATED CONTENT

Supporting Information

Supplementary data, as mentioned in the text. This material is available free of charge via the Internet at http://pubs.acs.org. CCDC 877662 contains the supplementary crystallographic data for this paper. These data can be obtained free of charge from The Cambridge Crystallographic Data Centre via www.ccdc.cam.ac.uk/data_request/cif.

AUTHOR INFORMATION

Corresponding Author

*E-mail: mercuri@unica.it. Phone: +39 070 6754486. Fax: +39 070 6754456.

Notes

The authors declare no competing financial interest.

ACKNOWLEDGMENTS

This work is supported by the EU (COST Action D35-WG-0011-005); Regione Autonoma della Sardegna, L.R. 7-8-2007, Bando 2009, CRP-17453 Project "Nano Materiali Multifunzionali per Applicazioni nell'Elettronica Molecolare"; Spanish Ministerio de Economía y Competitividad (Projects Consolider-Ingenio in Molecular Nanoscience CSD2007-00010 and CTQ-2011-26507); and the Generalitat Valenciana (Project Prometeo2009/095).

REFERENCES

(1) (a) Coronado, E.; Day, P. *Chem. Rev.* **2004**, *104*, 5419. (b) Enoki, T.; Miyazaki, A. *Chem. Rev.* **2004**, *104*, 5449. (c) Kobayashi, H.; Cui, H.; Kobayashi, A. *Chem. Rev.* **2004**, *104*, 5265. (d) Mercuri, M. L.; Deplano, P.; Serpe, A.; Artizzu, F. Multifuctional Materials of interest in Molecular Electronics. *Chapter in Handbook of Multifunctional Molecular Materials*Ouahab, L., ed.; Pan Stanford Publishing, 2011

(2) (a) Graham, A. W.; Kurmoo, M.; Day, P. *J. Chem. Soc., Chem. Commun.* **1995**, 2061. (b) Kurmoo, M.; Graham, A. W.; Day, P.; Coles, S. J.; Hursthouse, M. B.; Caulfield, J. L.; Singleton, J.; Pratt, F. L.; Hayes, W. *J. Am. Chem. Soc.* **1995**, *117*, 12209. (c) Coronado, E.; Curreli, S.; Gimenez-Saiz, C.; Gómez-García, C. J. *J. Mater. Chem.* **2005**, *15*, 1429. (d) Coronado, E.; Curreli, S.; Giménez-Saiz, C.; Gómez-García, C. J. *Synth. Met.* **2005**, *154*, 245. (e) Prokhorova, T. G.; Buravov, L. I.; Yagubskii, E. B.; Zorina, L. V.; Khasanov, S. S.; Simonov, S. V.; Shibaeva, R. P.; Korobenko, A. V.; Zverev, V. N. *CrystEngComm* **2011**, *13*, 537. (f) Akutsu, H.; Akutsu-Sato, A.; Turner, S. S.; Le Pevelen, D.; Day, P.; Laukhin, V.; Klehe, A.; Singleton, J.; Tocher, D. A.; Probert, M. R.; Howard, J. A. K. *J. Am. Chem. Soc.* **2002**, *124*, 12430. (g) Coronado, E.; Curreli, S.; Giménez-Saiz, C.; Gómez-García, C. J. *Inorg. Chem.* **2012**, *51*, 1111.

(3) (a) Coronado, E.; Galán-Mascarós, J. R.; Gómez-García, C. J.; Laukhin, V. *Nature* **2000**, *408*, 447. (b) Alberola, A.; Coronado, E.; Galán-Mascarós, J. R.; Giménez-Saiz, C.; Gómez-García, C. J. *J. Am. Chem. Soc.* **2003**, *125*, 10774. (c) Coronado, E.; Galán-Mascarós, J. R.; Gómez-García, C. J.; Martínez-Ferrero, E.; van Smaalen, S. *Inorg. Chem.* **2004**, *43*, 4808. (d) Alberola, A.; Coronado, E.; Galán-Mascarós, J. R.; Giménez-Saiz, C.; Gómez-García, C. J.; Martínez-Ferrero, E.; Murcia-Martinez, A. *Synth. Met.* **2003**, *135*, 687.

(4) (a) Calatayud, M. L.; Sletten, J.; Julve, M.; Castro, I. *J. Mol. Struct.* **2005**, *741*, 121. (b) Castro, I.; Sletten, J.; Faus, J.; Julve, M.; Journaux, Y.; Lloret, F.; Alvarez, S. *Inorg. Chem.* **1992**, *31*, 1889.

(5) (a) Castan, P.; Deguenon, D. *Acta Cryst. Sect. C* **1991**, *47*, 2656. (b) Carranza, J.; Sletten, J.; Brennn, C.; Lloret, F.; Cano, J.; Julve, M. *Dalton Trans.* **2004**, 3997. (c) Wang, C.-C.; Yang, C.-H.; Lee, G.-H. *Inorg. Chem.* **2002**, *41*, 1015.

(6) (a) Coronado, E.; Curreli, S.; Giménez-Saiz, C.; Gómez-García, C. J.; Deplano, P.; Mercuri, M. L.; Serpe, A.; Pilia, L.; Faulmann, C.; Canadell, E. *Inorg. Chem.* **2007**, *46*, 4446. (b) Gómez-García, C. J.; Coronado, E.; Curreli, S.; Giménez-Saiz, C.; Deplano, P.; Mercuri, M. L.; Pilia, L.; Serpe, A.; Faulmann, C.; Canadell, E. *Chem. Commun.* **2006**, 4931.

(7) (a) Speier, G.; Speier, E.; Noll, B.; Pierpont, C. G. *Inorg. Chem.* **1997**, *36*, 1520. (b) Plater, M. J.; Foreman, M. R., St.; Howie, R. A. *J. Chem. Crystal.* **1998**, *28*, 653. (c) Castro, I.; Calatayud, M. L.; Lloret, F.; Sletten, J.; Julve, M. *J. Chem. Soc., Dalton Trans.* **2002**, 2397. (d) Wang, C.-C.; Tseng, S.-M.; Lin, S.-Y.; Liu, F.-C.; Dai, S.-C.; Lee, G.-H.; Shih, W.-J.; Sheu, H.-H. *Cryst. Growth Des.* **2007**, *7*, 1783.

(8) (a) Abbati, G. L.; Cornia, A.; Babretti, A. C. *Acta Cryst. Sect. C* **1999**, *55*, 2043. (b) Wang, C.-C.; Yang, C.-H.; Tseng, S.-M.; Lee, G.-H.; Chiang, Y.-P.; Sheu, H.-S. *Inorg. Chem.* **2003**, *42*, 8294.

(9) (a) Cornia, A.; Fabretti, A. C.; Giusti, A.; Ferraro, F.; Gatteschi, D. *Inorg. Chim. Acta* **1993**, *212*, 87. (b) Ghoshal, D.; Ghosh, A. K.; Ribas, J.; Mostafa, G.; Chaudhuri, N. R. *Cryst. Eng. Commun.* **2005**, *7*, 616.

(10) Wang, C.-C.; Kuo, C.-T.; Yang, J.-C.; Lee, G.-H.; Shih, W.-J.; Sheu, H.-S. *Cryst. Growth Des.* **2007**, *7*, 1476.

(11) (a) Gavilan, E.; Audebrand, N. *Polyhedron* **2007**, *26*, 5533. (b) Maji, T. K.; Konar, S.; Mostafa, G.; Zangrando, E.; Lu, T.-H.; Chaudhuri, N. R. *J. Chem. Soc., Dalton Trans.* **2003**, 171.

(12) Maji, T. K.; Ghoshal, D.; Zangrando, E.; Ribas, J.; Chaudhuri, N. R. *Cryst. Eng. Commun.* **2004**, *6*, 623.

(13) de Paula, E. E. B.; Visentin, L. C.; Yoshida, M. I.; De Oliveira, L. F. C.; Machado, F. C. *Polyhedron* **2011**, *30*, 213.

(14) Brouca-Cabarrecq, C.; Trombe, J. C. *Inorg. Chim. Acta* **1992**, *191*, 227.

(15) (a) Curreli, S.; Deplano, P.; Faulmann, C.; Mercuri, M. L.; Pilia, L.; Serpe, A.; Coronado, E.; Gómez-García, C. J. *Inorg. Chim. Acta* **2006**, *359*, 1177. (b) Artizzu, F.; Deplano, P.; Pilia, L.; Serpe, A.; Marchiò, L.; Bernot, K.; Mercuri, M. L. *Inorg. Chim. Acta* **2011**, *370*, 474.

(16) (a) Sletten, J.; Daraghmeh, H.; Lloret, F.; Julve, M. *Inorg. Chim. Acta* **1998**, *279*, 127. (b) Wang, C. C.; Lin, H. W.; Yang, C. H.; Liao, C. H.; Lan, I. T.; Lee, G. H. *New J. Chem.* **2004**, *28*, 180. (c) West, R.; Ito, M. *J. Am. Chem. Soc.* **1963**, *85*, 2586.

(17) Gmelin, L. *Justus Liebigs Ann. Chem.* **1841**, *37*, 58−65.

(18) Bain, G. A.; Berry, J. F. *J. Chem. Educ.* **2008**, *85*, 532.

(19) Otwinowski, Z.; Minor, W. *DENZO-SCALEPACK*, Processing of X-ray Diffraction Data Collected in Oscillation Mode. In *Methods Enzymology, Macromolecular Crystallography, part A*; Carter, C. W., Jr., Sweet, R. M., Eds.; Academic Press: New York, 1997; Vol. *276*, p 307.

(20) Altomare, A.; Burla, M. C.; Camalli, M.; Cascarano, G.; Giacovazzo, C.; Guagliardi, A.; Moliterni, A. G. G.; Polidori, G.; Spagna, R. *J. Appl. Crystallogr.* **1999**, *32*, 115.

(21) Farrugia, L. J. *J. Appl. Crystallogr.* **1999**, *32*, 837.

(22) Sheldrick, G. M. *SHELX-97*, an integrated system for solving and refining crystal structures from diffraction data, University of Götingen, Germany, 1997.

(23) Blessing, R. H. *J. Appl. Crystallogr.* **1997**, *30*, 421.
(24) (a) Doan, L. M.; Fatiadi, A. J. *Angew. Chem.* **1982**, *94*, 649. (b) Doan, L. M.; Fatiadi, A. J. *J. Electroanal. Chem.* **1982**, *135*, 193.
(25) Fabre, P. L.; Dumestre, F.; Soula, B.; Galibert, A. M. *Electrochim. Acta* **2000**, *45*, 2697.
(26) Dumestre, F.; Soula, B.; Galibert, A. M.; Fabre, P. L.; Bernardinelli, G.; Donnadieu, B.; Castan, P. *J. Chem. Soc., Dalton Trans.* **1998**, 4131.
(27) Soula, B.; Galibert, A. M.; Donnadieu, B.; Fabre, P. L. *Dalton Trans.* **2003**, 2449.
(28) Mercuri, M. L.; Deplano, P.; et al. *Coord. Chem. Rev.* **2010**, *254*, 1419−1433.
(29) Horiuchi, S.; Tokunaga, Y.; Giovannetti, G.; Picozzi, S.; Itoh, H.; Shimano, R.; Kumai, R.; Tokura, Y. *Nature* **2009**, *463*, 789.
(30) West, R.; Ito, M. *J. Am. Chem. Soc.* **1963**, *85*, 2580.
(31) Steiner, T. *Angew. Chem., Int. Ed.* **2002**, *41*, 48.
(32) (a) Curély, J. *Europhys. Lett.* **1995**, *32*, 529. (b) Curély, J. *Phys. B* **1998**, *245*, 263.
(33) Delgado, F. S.; Kerbellec, N.; Ruiz-Pérez, C.; Cano, J.; Lloret, F.; Julve, M. *Inorg. Chem.* **2006**, *45*, 1012.
(34) O'Connor, C. J. *Prog. Inorg. Chem.* **1982**, *29*, 203.
(35) (a) Desplanches, C.; Ruiz, E.; Rodríguez-Fortea, A.; Alvarez, S. *J. Am. Chem. Soc.* **2002**, *124*, 5197. (b) Desplanches, C.; Ruiz, E.; Alvarez, S. *Chem. Commun.* **2002**, 2614.